9TH AUSTRALASIAN HEAT AND MASS TRANSFER CONFERENCE - 9AHMTC
MONASH UNIVERSITY, Melbourne, Victoria, Australia, November 2-4, 2011

Optimization of the Air Gap Spacing In a Solar Water Heater with Double Glass Cover

M. AL-Khaffajy[1] and R. Mossad[2]

Faculty of Engineering and Surveying, University of Southern Queensland, QLD 4350, AUSTRALISA
MarwaanAwadHamad.Al-khaffajy@usq.edu.au

ABSTRACT

A parametric study has been conducted in a solar water heater with double glass cover, in order to minimize heat losses. The air gap spacing between the absorber and the lower glass cover (L_1) and between the two glass covers (L_2) for the system with 0.7 m x 1.35 m absorber area were varied within the range of 15-50 mm to investigate which combination of gap sizes (L_1, L_2) would result in minimum total heat losses i.e. including radiation and convection losses. Three-dimensional CFD models have been developed using ANSYS 13.0-FLUENT software. The continuity, momentum and energy equations have been solved, in steady state condition, using pressure-based type solver. A realizable k-ϵ turbulent model has been used, and surface to surface radiation was included. The results showed that when the gap size was small the heat loss through the gap was mainly due to conduction while as the gap size increased in most cases the velocity of the air in the gap increased which increased the convection contribution to the heat loss. The optimum combinations for the present case have been found to be 40, 25 mm, since the overall heat loss was found to have the lowest heat loss of 213.18 W.

1. INTRODUCTION

The massive increase in the price of fossil fuel and its negative environmental impact have led to increased research involving cheap and clean sources of energy such as solar energy. The use of solar energy has been growing in electricity generation, air conditioning and water heating. An important and costly use, environmentally and economically, occurs in the production of domestic hot water. Fourteen per cent of energy usage by households is for water heating [3]. An economic and efficient system is required to encourage households to use solar water heating.

Solar flat plate collectors are used for producing domestic hot water. Integrated collectors are a type of the flat plate collectors characterized by incorporating the collection of the solar energy part and the storage of hot water in one unit [9]. Integrating the collector and storage tank in one part reduces the cost of the system as there are no connection pipes and only a small area is needed for installation [5, 6]. The integrated collector system consists of a black surface which absorbs the solar radiation and transfers the heat to the fluid, a glass cover to reduce convection and radiation losses, a storage tank into which the water flows when it is used or gets stored when not in use and insulation in the back and side to reduce heat losses (see figure 1).

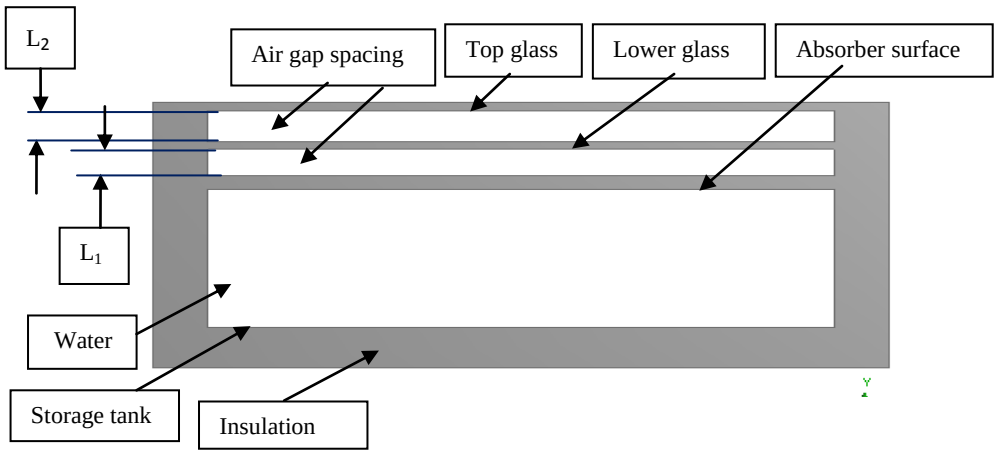

Figure 1. Cross section of the integrated collector storage solar water heater system

Previous studies showed that the performance of the integrated collector system can be improved by enhancing the heat transfer between the absorber surface and the storage water and reducing heat loss. Kumar & Rosen [8] used a corrugated absorber surface to enhance the heat transfer between the absorber and the storage water. Kumar & Rosen [9] investigated five strategies for reducing top heat loss. The 100L tank capacity model and 1 m^2 absorber area was used to assess five cases: (1) single glass cover without night insulation, (2) single glass cover with night insulation cover; (3) double glass cover without night insulation cover; (4) transparent insulation with single glass cover and (5) insulating baffle plate with single glass cover. They found that case three provided the greatest thermal performance while case 5 has the lowest thermal efficiency.

In solar flat plate collectors, the overall heat loss coefficient (U_t) can be evaluated using the available empirical equations. According to Duffie and Beckman [4], Klein (1979) developed a useful empirical equation for calculating the top heat loss coefficient (U_t).

$$U_t = \left[\frac{N}{\frac{C}{T_{pm}}\left(\frac{T_{pm}-T_a}{N+f}\right)^e}+\frac{1}{h_w}\right]^{-1} + \frac{\sigma\left(T_{pm}+T_a\right)\left(T_{pm}^{\,2}+T_a^{\,2}\right)}{\left(\varepsilon_p+0.00591\,Nh_w\right)^{-1}+\frac{2N+f-1+0.133\varepsilon_p}{\varepsilon_g}-N} \quad (1.1)$$

$$f = \left(1+0.098h_w-0.1166h_w\varepsilon_p\right)(1+0.07866N) \quad (1.1a)$$

$$C = 520(1-0.000051\beta^2) \text{ for } 0<\beta<70^o.\text{ for } 70^o<\beta<90^o, \text{use } \beta = 70^o$$

$$e = 0.430\left(1-\frac{100}{T_{pm}}\right) \quad (1.1b)$$

Where
h_w: Convective heat transfer coefficient due to wind
N: Number of glass covers
T_a: Ambient temperature
T_{pm}: Absorber temperature
β : Collector tilt angle
ε_g : Emissivity of glass
ε_p: Emissivity of absorber

Akhtar and Mullick [1] proposed a set of correlations to compute the mean temperature of the glass cover.

$$T_2 = \left(f_2T_{pm}+CT_a\right)/\left(1+f_2\right) \quad (1.2)$$

$$f_2 = \frac{\left[\left\{12\times10^{-8}\left(T_a+0.2T_{pm}\right)^3+h_w\right\}^{-1}+0.3L_{g2}\right]\left(0.7-0.26\varepsilon_p\right)}{\left[6\times10^{-8}\left(\varepsilon_p+0.028\right)\left(T_{pm}+0.5T_a\right)^3+0.6L_1^{-0.2}\left\{\left(T_{pm}-T_a\right)\cos\beta\right\}^{0.25}\right]^{-1}} \quad (1.2a)$$

Where C = 1 for Ts = Ta and $C = \frac{\left(\frac{T_s}{T_a}+h_w/3.5\right)}{\left(1+h_w/3.5\right)}$ for Ts = 0.0552 Ta1.5.

$$T_1 = \left(f_1T_{pm}+T_2\right)/\left(1+f_1\right) \quad (1.3)$$

$$f_1 = \frac{[3.1\sigma(T_2+\Delta_o)^3+0.8(\Delta_o\cos\beta)^{0.25}L_2^{-0.2}]^{-1}+0.3L_{g1}}{\left[3.45\sigma\varepsilon_p\left(T_{pm}-\Delta_i\right)^3+0.8(\Delta_i\cos\beta)^{0.25}L_1^{-0.2}\right]^{-1}} \quad (1.3a)$$

$$\Delta_i = \left(2-\varepsilon_p\right)\left(T_{pm}-T_2\right)/6 \quad (1.3b)$$

$$\Delta_o = \left(1+\varepsilon_p\right)\left(T_{pm}-T_2\right)/6 \quad (1.3c)$$

Where:
L_1: Air gap spacing between absorber plate and the first glass cover
L_2: Air gap spacing between the first and second glass
$L_{g1, g2}$: Thickness of the first and second glass
T_1: Lower glass temperature
T_2: Top glass temperature

The top heat loss coefficient (U_t) evaluated based on the mean temperature of each glass cover (T_1 and T_2) estimated from the above correlations [1].

Manz [10] investigated numerically the convective heat flow through an air layer in cavities of facade elements. It is known that natural convection heat retransfer coefficient depends on Rayleigh number. The Rayleigh number defined as $\left(R_{aL} = \frac{g\,L^3\beta\,(T_h-T_c)}{\alpha\,v}\right)$ was varied between 1000 and 10^6. It was changed by altering the temperature difference$(T_h - T_c)$ between the walls surrounding the air or the distance between walls (L). The result of Manz's study showed that increasing the Rayleigh number results in an increase in the velocity of the air between the two glasses. Mossad [11] investigated the effect of the air gap spacing of double glassed doors in closed refrigerated vertical display cabinets. The results showed that when the size of the air gap was very small, the heat transfer was

mainly due to conduction: as the gap spacing increased, air starts to move due to natural convection which leads to an increase in the convective heat loss.

It is necessary to optimize the air gap spacing (L_1 and L_2) in the integrated collector system with double glass cover, since they have an effect on the thermal performance as well as cost and weight of the system. For the integrated collector system with a single glass cover, the optimum air gap spacing between the absorber and the glass cover was found to be 40 mm [2]. To the best knowledge of the authors, the optimum air gap spacing in the integrated collector storage solar water heater system with double glass cover has not been investigated. The present study will investigate numerically the optimum size of air gaps (L_1 and L_2) in the integrated collector storage solar water heater system.

2. MATHEMATICAL MODEL

To predict the heat losses from the solar collector, the velocity and temperature of the air in the gap spacing and the temperature of the top and bottom glass covers need to be evaluated since the heat loss depends on these values. The governing equations for the flow according to Raisee and Hejazi [12], for steady, incompressible and turbulent flow can be written in abbreviated form as:

Continuity equation

$$\frac{\partial U_j}{\partial x_j} = 0 \qquad (2.1)$$

Momentum equation

$$\frac{\partial U_j U_i}{\partial x_j} = -\frac{1}{\rho}\frac{\partial p}{\partial x_i} + \frac{\partial}{\partial x_j}\left(\upsilon \frac{\partial U_i}{\partial x_j} - \overline{u_i u_j}\right) + f_i \qquad (2.2)$$

Energy equation

$$\frac{\partial (U_j T)}{\partial x_j} = \frac{\partial}{\partial x_j}\left(\frac{\upsilon}{Pr}\frac{\partial T}{\partial x_j} - \overline{u_j \theta}\right) \qquad (2.3)$$

Where:
f_i: Body force
P: Air pressure
U_i: air mean velocity component (u, v, w)
$u_i u_j$: Reynolds stress tensor
x_i: Cartesian coordinates (x, y, z)
$\overline{u_j \theta}$: Turbulent heat flux tensor
Pr: Turbulent Prandtl number
υ: Kinematic viscosity of air

The above equations are non-linear partial differential equations and the analytical solution is impossible except for very simple cases, but these equations can be solved numerically. The present study used FLUENT software that uses finite volume approach to solve the continuity, momentum and energy equation. The pressure-based type solver was used. The effect of gravity was included considering full buoyancy effect. The variation of the properties of air with temperature has been included by using incompressible ideal gas equation for estimating the density and kinetic theory equation for specific heat, thermal conductivity and viscosity.

The Realizable k-ϵ turbulence model has been used. The flow near the walls was treated by using Non-Equilibrium wall function and the velocity-pressure coupling was treated by using the SIMPLE algorithm and a first order upwind scheme for Momentum, Turbulent Kinetic Energy and Turbulence Dissipation. For the residual, 10^{-4} was used as the accuracy of solution for all terms: x-velocity, y-velocity, z-velocity, kinetic energy, epsilon and continuity, except for the energy, which was 10^{-8}.

3. CFD SIMULATION

Steady 3D CFD models for the absorber with the double glass cover have been developed to evaluate the radiation and convection heat losses. The lower gap L_1 was kept constant at 15, 25 and 40 mm while the top gap L_2 was changed to 15, 25, 35 and 50 mm. The objective was to find the optimum combination of L_1 and L_2 which result in minimum total heat loss.

The boundary conditions on the side-wall and top-glass cover was taken as convection with a heat transfer coefficient of 10 W/(m^2 K) to an ambient temperature of 290 K and radiation to the sky at a temperature which was taken according to Akhtar & Mullick [1] as $0.0552\ Ta^{1.5}$. A constant temperature of 355 K was assumed for the absorber surface in all cases. The collector angle was chosen to be 45^o (see figure 2). The absorber surface was made of metallic nickel chrome (M-N-chrome) with 5 mm thickness, 0.7m x 1.35 m surface area and the glass thickness was chosen to be 3 mm, the side walls were made of wood with 50 mm thickness. The physical properties adopted in the simulation of these materials are given in table 1.

Material name	Density (ρ) kg/m^3	Specific heat (C_p) J/ (kg. K)	Thermal conductivity (k) W/(m. K)	Emittance (ϵ)
M-N-chrome	7865	460	19	0.94
Glass	2800	800	0.81	0.93
Wood	700	2310	0.173	0.9

Table 1. Physical properties of material

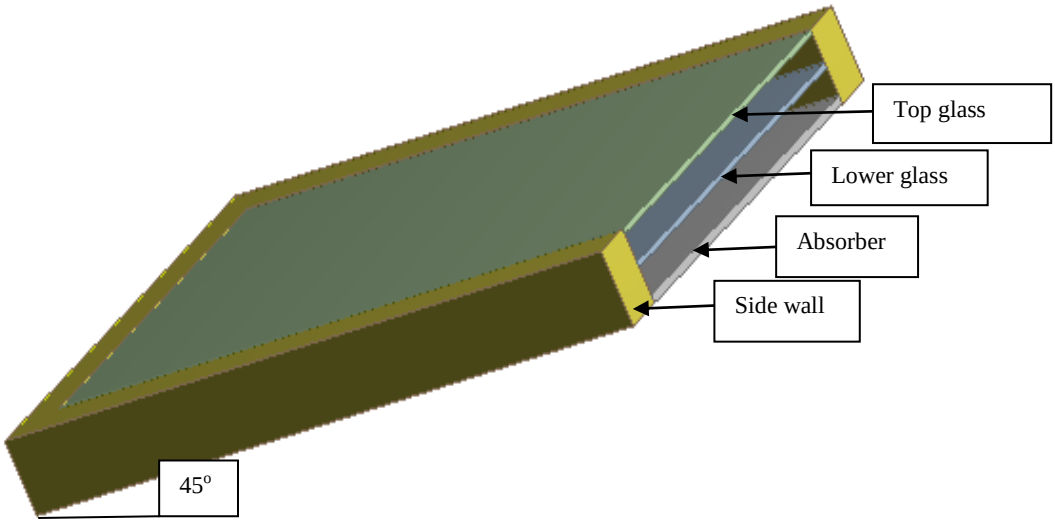

Figure 2. 3D model of the air spacing of the integrated collector system

The geometry was modelled using ANSYS 13.0. To validate the grid dependency, three computational grids have been developed for the model with L_1 equals 25 mm and L_2 50 mm; 100,000 elements, 162,000 elements and 227,500 elements. The element shape is hexahedral for all models. The 162,000 elements and 227,500 elements provided the same result which had 1-1.2% difference from the results of the 100,000 model. Therefore; the number of elements was kept in the range of 162,000-227,500 for all other models.

Radiation between surfaces and to the sky has been considered. A surface to surface radiation model was used, ignoring the effect of the medium between surfaces. The radiation process was started by estimating the view factors between the surfaces. In every ten iterations throughout the solution, the radiosity of the surfaces has been updated based on the new surfaces' temperature through another iterative process to include the heat transfer due to radiation more accurately.

4. RESULTS

Combinations of twelve cases modelled as lower gap, L_1, and top gap, L_2, were changed. L_1 was kept constant at 15, 25 and 40 mm while L_2 was changed to 15, 25, 35 and 50 mm. The velocity of the air in the middle of the top and lower gaps along the collector is given in figures 3a, 3b, 4a, 4b, 5a and 5b. The results showed that in most cases the velocity becomes higher as the gap spacing increases, however in cases, 3-a, 4-a, the changes did not follow the same pattern.

Temperatures in a line in the middle of the top glass and the lower glass along the collector are given in figures 6a, 6b, 7a, 7b, 8a and 8b. The top glass temperature always dropped as the gap size L_2 increased, while temperature increased in the lower glass as L_2 increased with the exception of the case when L_1=15 mm and L_2=50 mm when the temperature dropped in comparison to the previous values of L_2. Another observation is that the temperature of the top and lower glass, when L_1 = 25 and 40 mm for L_2 = 35 and 50 mm, were very close to each other.

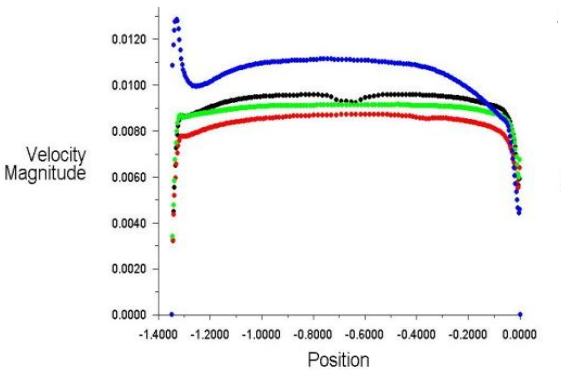

Figure 3-a. Velocity in the middle of lower gap L_1=15 mm

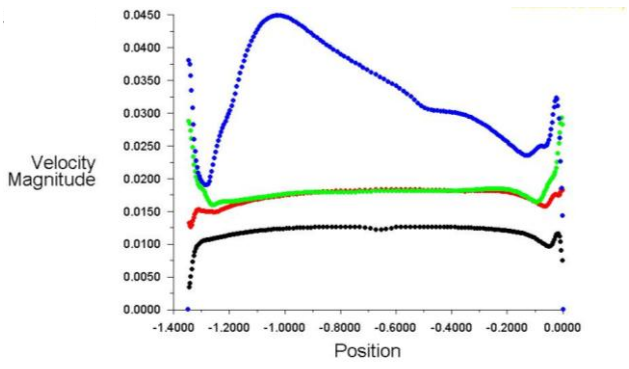

Figure 3-b. Velocity in the middle of top gap L_1=15 mm

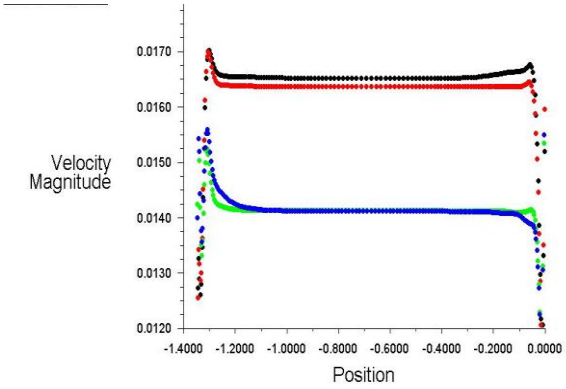

Figure 4-a. Velocity in the middle of lower gap L_1=25 mm

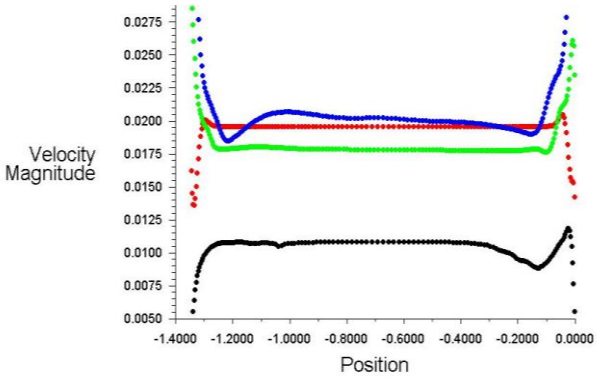

Figure 4-b. Velocity in the middle of top gap L_1=25 mm

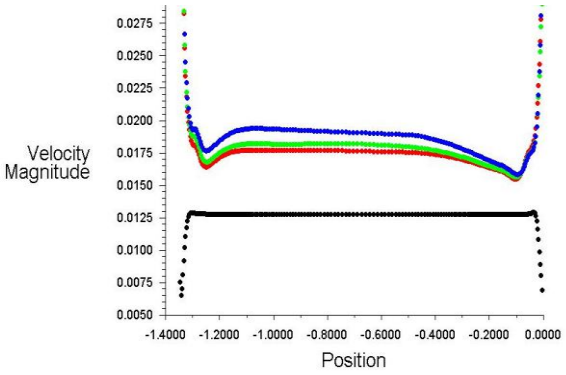

Figure 5-a Velocity in the middle of lower gap L_1=40 mm

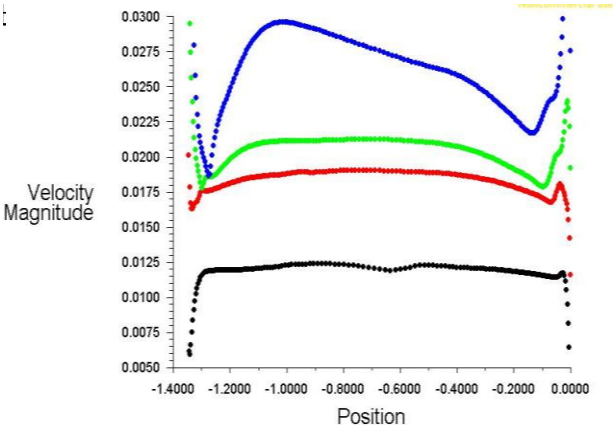

Figure 5-b Velocity in the middle of top gap L_1=40 mm

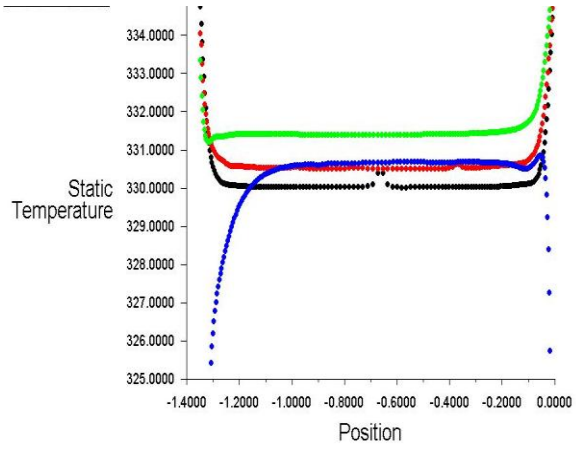

Figure 6-a. Temperature of lower glass for L_1=15 mm

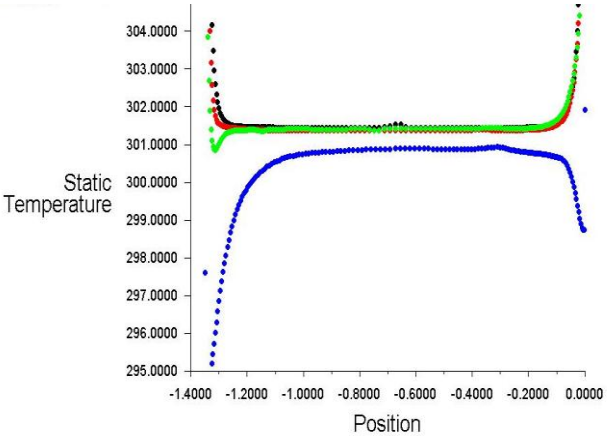

Figure 6-b. Temperature of top glass for L_1=15 mm

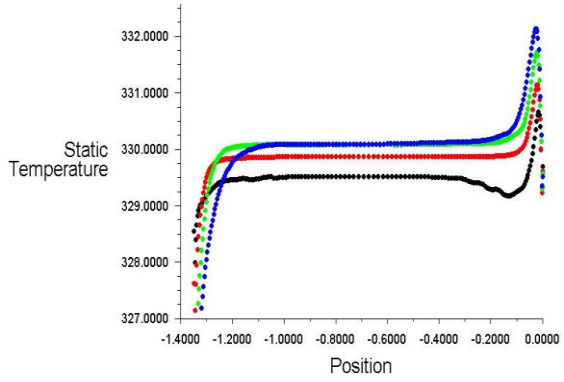

Figure 7-a. Temperature of lower glass for L_1=25 mm

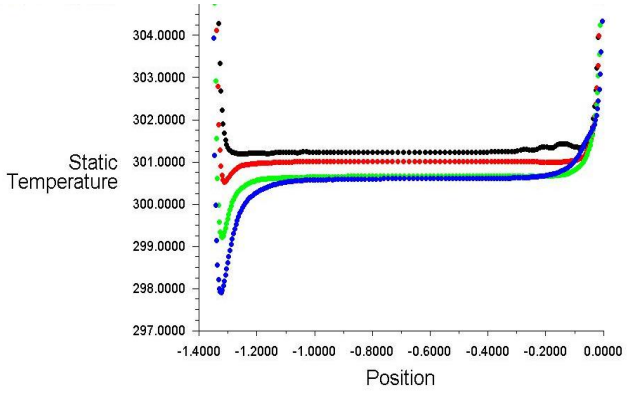

Figure 7-b. Temperature of top glass for L_1=25 mm

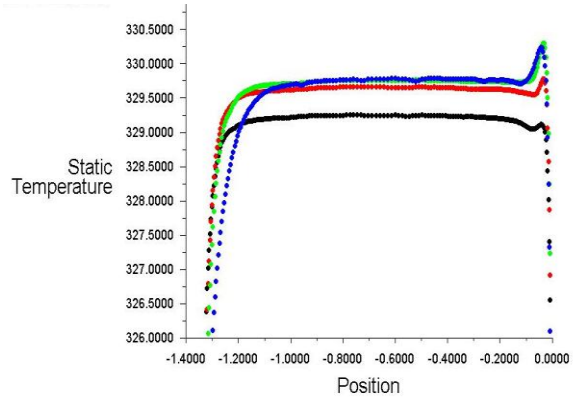

Figure 8-a. Temperature of lower glass for L_1=40 mm

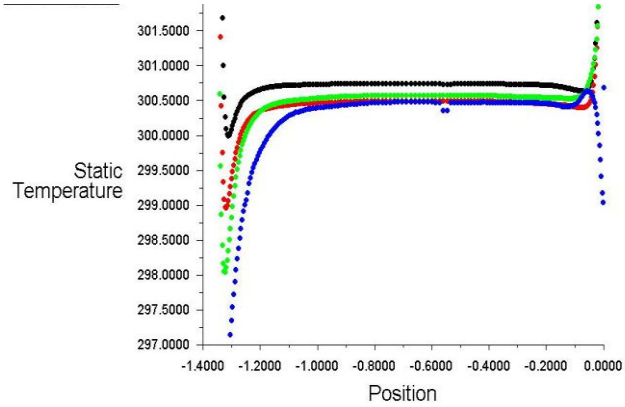

Figure 8-b. Temperature of top glass for L_1=40 mm

5. DISCUSSION

In the case when the lower gap L_1 was 15 mm, the lower glass temperature increased, 6-a as the top gap L_2 increased from 15 – 35 mm. This may be because the heat transfer within the top gap was dominated by conduction, as can be seen by the low air speeds, 3-b, and this enhanced the insulation effect. Another factor could be that most of the radiation from the absorber reached the lower glass due to its higher shape factor in comparison to the shape factor of the sides. When L_2 reached 50 mm, it helped the air to move at a higher speed, 3-b, and this caused cooling of the lower glass temperature, 6-a.

When L_1 was 25 and 40 mm as the top gap L_2 increased, the temperature of the lower glass in all cases increased, 7-a and 8-a. It is notable that the temperature increase rate was higher at the beginning and then decreased as the top gap L_2 increased. This may be because some natural convection started to take part in moving the heat (see figure 4-b and 5-b), which minimized the effect of the conduction mode. It is also noteworthy that as L_1 increased for all L_2 values, the lower glass temperature reduced due to increased radiation from the absorber reaching the side walls.

The convection current in the air gap is affected by the temperature difference across the gap and the size of the gap. As the size of the top gap L_2 increased, the temperature difference between the top glass and the lower glass increased which explains the increase in the air velocities within the gap, as shown in figures 4-b and 5-b. The Rayleigh number for these cases changed from 1.4 x 10^7 to 7.8 x 10^7, which indicate a fully turbulent flow, according to Kreith [7]. These results confirm Manz's [10] finding that increasing the Rayleigh number leads to increased velocity of the air in the gap.

In regards to the heat balance in the collector, the absorber surface is heated from the solar radiation which has been transmitted through the glass covers. This energy heats the water in the storage tank below the absorber and loses heat due to convection to the air in the lower gap, radiation to the lower-side walls (the side-wall surrounding the lower air gap spacing) and radiation to the lower glass cover. The lower glass cover loses heat due to convection to the air in the top gap and through radiation to the upper-side walls and to the top glass cover. The top glass cover loses heat due to convection to the ambient air and due to radiation to the sky. The heat loss from the top glass due to convection for all cases is given in figure 9, and the heat loss due to radiation to the sky is given in figure 10.

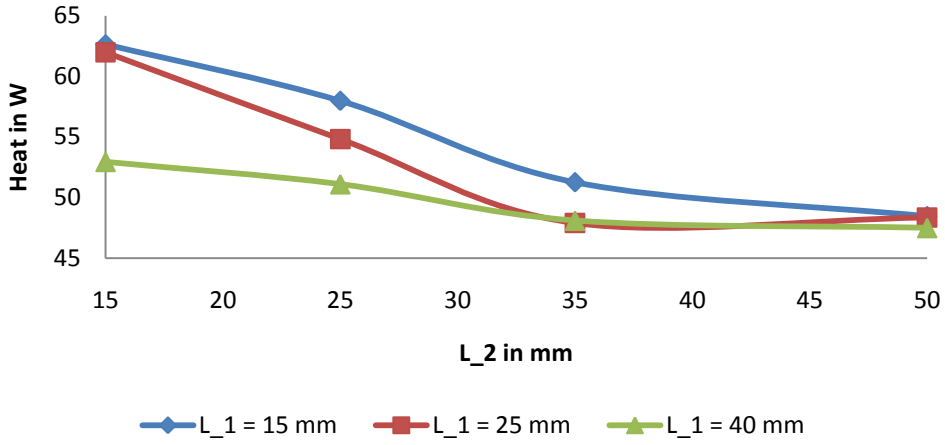

Figure 9. Convection heat transfer from top glass

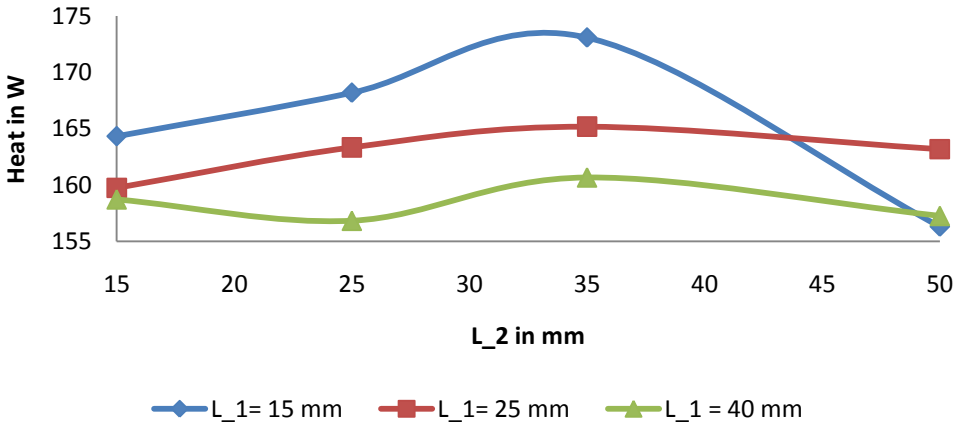

Figure 10. Radiation heat transfer from top glass

It is important to note that heat loss due to convection from the top glass for all L_1 values dropped as L_2 increased until it levelled out at the higher values of L_2. Radiation heat loss for all L_1 cases did increase at the beginning then reached a maximum and started to decrease as L_2 increased. The radiation heat loss depends on the temperature of the top glass in comparison to the sky temperature, while the convection heat loss depends on the temperature difference between the top glass and the ambient temperature. A small difference in the top glass temperature affects the radiation component in a more obvious way since it depends on T^4. The total of these two components for all cases are given in figure 11.

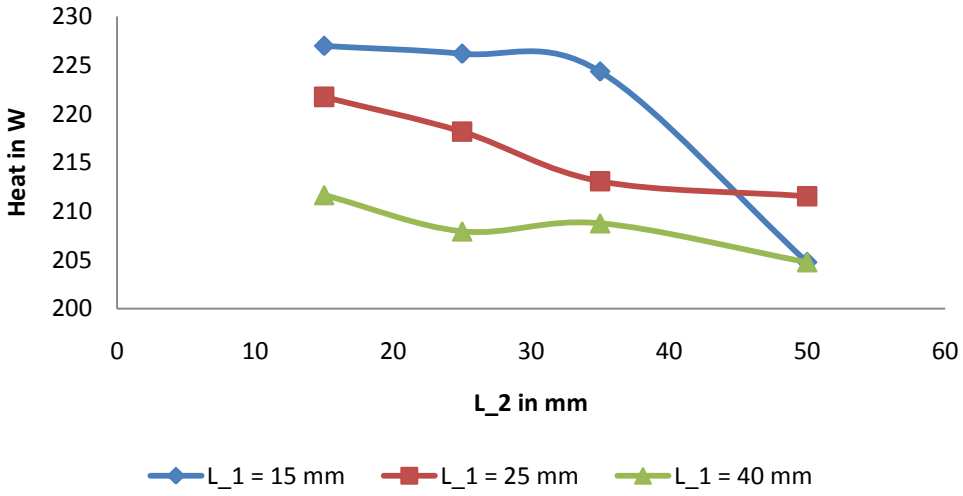

Figure 11. Total heat loss from top glass

It is apparent that the total heat lost due to convection and radiation from the top glass decreased as L_2 increased for all L_1 cases. However, to identify the optimum air gap spacing, it is important to consider the total heat loss from the double glassed solar heat collector which equals to the total top glass heat loss due to convection and radiation plus the heat lost through the side walls; both the lower and top parts: these are given in figure 12. The heat loss from the side walls of the gap, including the convection and the radiation parts, depends on their area and their temperature. From figure 12, one can see that the optimum case is the combination of L_1= 40 mm and L_2 =25 mm which gives a minimum heat loss of 213.18 W.

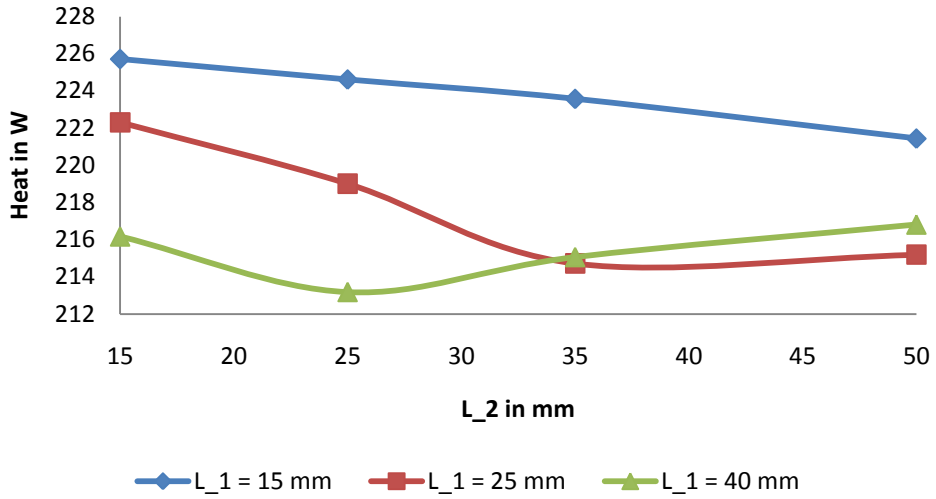

Figure 12. Total heat loss from top and side-wall

6. CONCLUSION

To minimize the heat losses from the solar water heater with double glassed cover, a parametric study was conducted to identify the optimum air gap spacing. ANSYS 13.0-FLUENT was used to solve the flow governing equations. The size of air gaps between the absorber and the lower glass cover (L_1) and between the lower and top glass cover (L_2) were varied in the range of 15 -50 mm to identify the combination (L_1, L_2) that provides the minimum heat losses. The result shows that the lowest heat loss can be achieved in the combination of L_1 = 40 mm and L_2 =25 mm which gave a heat loss of 213.18 W.

REFERENCES

[1] Akhtar N. & S.C. Mullick (2007) Computation of glass-cover temperatures and top heat loss coefficient of flat-plate solar collectors with double glazing. *Energy*, 32(7), 1067-1074.

[2] Chen Z., Gu M., Peng D., Peng C. & Wu Z. (2010) A numerical study on heat transfer of high efficient solar flat-plate collectors with energy storage. *International Journal of Green Energy*, 7(3), 326-336.

[3] Department of Energy, US (2010) Where Does My Money go?, viewed 28 April 2011, <http://www.energystar.gov/index.cfm?c=products.pr_pie>.

[4] Duffie, J.A. and W.A. (2006) Beckman, Solar engineering of thermal processes, 3rd Edition, New Jersey: John Wiliam & Sons, INC

[5] Gertzos K.P. Caouris Y.G. & Panidis T. (2010) Optimal design and placement of serpentine heat exchangers for indirect heat withdrawal, inside flat plate integrated collector storage solar water heaters (ICSSWH). *Renewable Energy*, 35(8), 1741-1750.

[6] Khalifa A.J.N. & Abdul Jabbar R.A. (2010) Conventional versus storage domestic solar hot water systems: A comparative performance study. *Energy Conversion and Management*, 51(2), 265-270.

[7] Kreith, F. (2010) Principles of heat transfer, 7th Edition, SI ed. ed, ed. R.M. Manglik and M. Bohn, Clifton Park NY: Nelson Engineerng. p cm.

[8] Kumar R. & Rosen M.A. (2010) Thermal performance of integrated collector storage solar water heater with corrugated absorber surface. *Applied Thermal Engineering*, 30(13), 1764-1768.

[9] Kumar R. & Rosen M.A. (2010) Comparative performance investigation of integrated collector-storage solar water heaters with various heat loss reduction strategies. *International Journal of Energy Research*.

[10] Manz H. (2003) Numerical simulation of heat transfer by natural convection in cavities of facade elements. *Energy and Buildings*, 35(3), 305-311.

[11] Mossad, R. (2006) Numerical simulation to optimize the design of double glazed doors for closed refrigerated vertical display cabinets. In *Proc. 13th International Heat Transfer Conference IHTC-13*. Redding, CT, USA: Begell House Inc, August.

[12] Raisee, M. & Hejazi S.H. (2007) Application of linear and non-linear low-Re k-[epsilon] models in two-dimensional predictions of convective heat transfer in passages with sudden contractions. *International Journal of Heat and Fluid Flow*, 28(3), 429-440.